Maltogenic α-amylase hydrolysis of wheat starch granules: mechanism and relation to starch retrogradation

Zhai, Yitan; Li, Xiaoxiao; Bai, Yuxiang; Jin, Zhengyu; Svensson, Birte

Published in:
Food Hydrocolloids

Link to article, DOI:
10.1016/j.foodhyd.2021.107256

Publication date:
2022

Document Version
Peer reviewed version

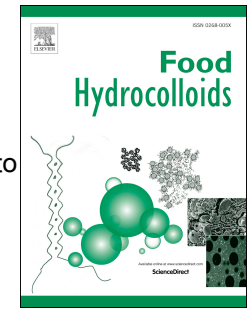

Maltogenic α-amylase hydrolysis of wheat starch granules: mechanism and relation to starch retrogradation

Yitan Zhai, Xiaoxiao Li, Yuxiang Bai, Zhengyu Jin, Birte Svensson

PII: S0268-005X(21)00672-X

DOI: https://doi.org/10.1016/j.foodhyd.2021.107256

Reference: FOOHYD 107256

To appear in: *Food Hydrocolloids*

Received Date: 16 July 2021

Revised Date: 17 September 2021

Accepted Date: 4 October 2021

Please cite this article as: Zhai, Y., Li, X., Bai, Y., Jin, Z., Svensson, B., Maltogenic α-amylase hydrolysis of wheat starch granules: mechanism and relation to starch retrogradation, *Food Hydrocolloids*, https://doi.org/10.1016/j.foodhyd.2021.107256.

CRediT authorship contribution statement

Yitan Zhai: Investigation, Writing, Validation, Conceptualization. **Xiaoxiao Li:** Review & editing. **Yuxiang Bai:** Review & editing, Project administration, Funding acquisition, Supervision. **Zhengyu Jin:** Funding acquisition. **Brite Svensson:** Review & editing.

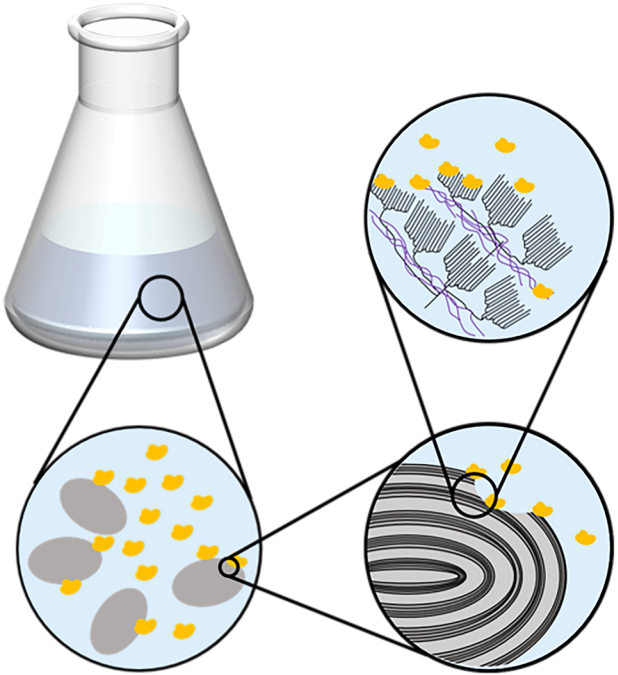

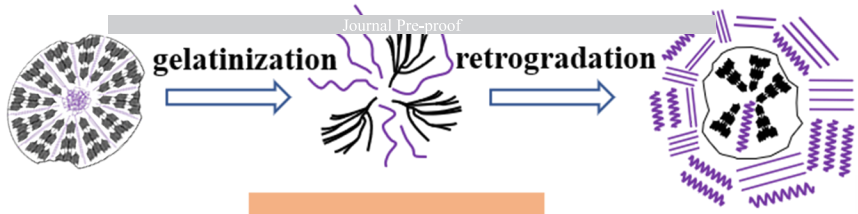

Retrogradation

MA amount	DH (%)
2.5 U/g	10.11±0.43^{e}
5 U/g	12.66±0.31^{d}
7.5 U/g	14.63±0.54^{c}
10 U/g	17.31±0.83^{b}
15 U/g	21.13±0.69^{a}

Degree of hydrolysis (DH)

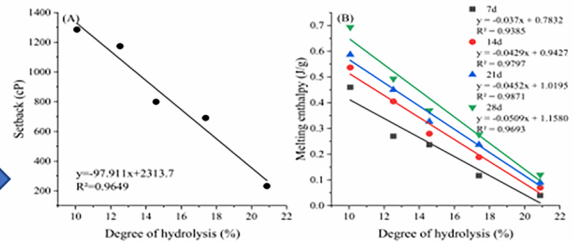

Retrogradation parameters displayed leaner correlation with DH

Wheat starch granule

Semi-crystalline growth ring

Amorphous growth ring

Maltogenic α-amylase (MA)

Amylose

Amylopectin

Maltogenic α-amylase hydrolysis of wheat starch granules: mechanism and relation to starch retrogradation

Yitan Zhai[a,b,c,e], Xiaoxiao Li[a,b,c,e], Yuxiang Bai[a,b,c,e,*], Zhengyu Jin[a,b,c,e], Birte Svensson[d,e]

[a]State Key Laboratory of Food Science and Technology, Jiangnan University, Wuxi, Jiangsu 214122, China;

[b]School of Food Science and Technology, Jiangnan University, Wuxi, Jiangsu 214122, China;

[c]Synergetic Innovation Center of Food Safety and Nutrition, Jiangnan University, Wuxi, Jiangsu 214122, China;

[d] Enzyme and Protein Chemistry, Department of Biotechnology and Biomedicine, Technical University of Denmark, DK-2800 Kgs. Lyngby, Denmark;

[e] International Joint Research Laboratory for Starch Related Enzyme, Jiangnan University, Wuxi, Jiangsu 214122, China;

[*]Corresponding authors

Dr. Yuxiang Bai

Associate Professor in State Key Laboratory of Food Science and Technology

E-mail address: ybai@jiangnan.edu.cn

Abstract: Enzymatic modification is an effective method to inhibit starch retrogradation. However, lack of quantification of relationships between enzymatic modification and starch retrogradation makes the enzymatic improvement unpredictable. In this study, maltogenic α-amylase (MA) was used to treat wheat starch granules to restrain retrogradation, aiming to elucidate the mechanism of MA hydrolysis on wheat starch granules and to establish a quantitative relationship between the degree of hydrolysis (DH) and retrogradation. Scanning electron microscopy and small angle X-ray scattering results showed that MA hydrolyzed starch granules by a "surface pitting" mode simultaneously acting on crystalline and amorphous regions. Debranching and high performance anion exchange chromatography analysis of MA-treated wheat starch granules demonstrated that the amount of short branches with degree of polymerization＜9 increased and the proportion of medium and long branches decreased. Importantly, the extent of impaired short- and long-term retrogradation of MA-treated starch was clearly linearly correlated with the DH. This finding provides a quantitative method for predicting the degree of retrogradation improvement by enzymatic modification.

Key words： maltogenic α-amylase; wheat starch granule; relationship; starch retrogradation

1. Introduction

As a crucial energy source for humans, starch is widely used as an ingredient in food industry. However, starchy foods are usually confronted with the challenge of staling, which makes its firmness increase and quality decrease (Fu, Chen, Luo, Liu, & Liu, 2015). This undesirable change is largely caused by the retrogradation of the starch component in foods. Therefore, physical (Adebowale & Lawal, 2003), chemical (Yang et al., 2021) and enzymatic (Li et al., 2016) methods have been attempted to inhibit starch retrogradation. Among these, enzymatic methods are receiving increasing attention as their safety, mild conditions and substrate specificity comply with "clean label" (Gui et al., 2021; Li et al., 2016; Park & Kim, 2021). Usually, the enzymatic modification of starch is conducted on the gelatinization systems as the semi-crystalline structures of native starch granules restrained the accessibility of amylase (Zhong et al., 2021). It is attractive in industry to keep the granular structure of starch from being completely destroyed during the enzymatic modification process, since it avoids that the modification system becomes too viscous to react in high concentrations. Besides, enzymes by directly treating raw starch granules could simplify the supply chains from production to final application circumstances.

Maltogenic α-amylase (MA) of glycoside hydrolase family 13 (GH13) (www.CAZy.org/) (Lombard, Golaconda Ramulu, Drula, Coutinho, & Henrissat, 2014) is commonly used in bakery as anti-staling agent and has recently been suggested to have the ability to modify native starch granules (Zhong et al., 2021). MA exhibits mainly an *exo*-action pattern, hydrolyzing α-1,4 glucosidic linkage successively with formation of maltose from the non-reducing chain ends. MA can also exhibit an *endo*-action pattern and hydrolyze internal glucosidic bonds releasing maltooligosaccharides (Dauter et al., 1999). Thus, MA can inhibit starch retrogradation by breaking down the cluster structure and shortening the branch chains of amylopectin (Grewal et al., 2015). The relationship has been investigated between structure and retrogradation of MA hydrolyzed waxy maize starch and potato starch (Chen et al., 2020; Grewal et al., 2015). These studies were based on gelatinization systems and reported no quantitative relationship between MA hydrolysis and starch retrogradation.

In the present study, to investigate the mechanism of MA hydrolysis on wheat starch granules and the relationship between MA hydrolysis and starch retrogradation, wheat starch granules were incubated with MA at sub-gelatinization temperature. The structural and retrogradation characteristics of MA treated wheat starch were analyzed and showed a good linear correlation between degree of hydrolysis

(DH) and starch retrogradation parameters. The findings provide an outstanding opportunity to quantify the degree of retrogradation, and hence the staling potential of enzymatically modified starchy foods such as bread, steamed bread and so on.

2. Materials and methods

2.1 Materials

Wheat starch was purchased from New Land Group (Xinxiang, China). Maltogenic α-amylase (> 11000U/g) from *Bacillus subtilis* and pullulanase were obtained from Novozymes (Denmark). Isoamylase (200 U/mL) from *Pseudomonas sp* was from Megazyme Co. Ltd (Wicklow, Ireland). All chemicals used were of reagent grade.

2.2 Enzyme modification of wheat starch

Wheat starch (50 g, dry basis) was suspended in 200 mL sodium acetate buffer (50 mM, pH5.0), and preheated on a water bath at 55℃ for 10 min. The enzymatic treatment was initiated by adding MA to the starch slurry at different dosages (2.5, 5, 7.5, 10, 15 U/g dry starch), conducted at 55°C with stirring (150 rpm) for 1 h and terminated by addition of 4 mL 1 M NaOH. The pH was adjusted back to 5.0 with 4 mL 1 M HCl followed by centrifugation (8,000×*g*, 10 min). The supernatant was collected for total carbohydrate analyses. The precipitate was washed thrice with deionized water and centrifuged as above to remove the remaining oligosaccharides. After that, the samples were dried at 40℃ overnight, ground in a mortar and passed through a 100-mesh sieve. The control sample was made by being subjected to the above process but with addition of denatured MA.

DH was calculated from the amount of total carbohydrate in the supernatant through the phenol-sulfuric acid method (DuBois, Gilles, Hamilton, Rebers, & Smith, 1956) according to the following equation:

$$DH(\%) = \frac{T_C \times 0.9}{M_S} \times 100 \quad (1)$$

where T_c is the amount of total carbohydrate in the supernatant; 0.9 is the conversion coefficient; M_s is the weight of native wheat starch (on dry basis).

2.3 Polarized light microscopy (PLM)

A light microscope (BX41TF, Olympus, Japan) was used to take polarized light images of all starch samples. Each sample was poured into deionized water to form a 1.5% (w/v) suspension and imaging at 200× magnification.

2.4 Scanning electron microscopy (SEM)

The morphological characteristics of all starch samples were observed using a SEM (SU8100, FESEM, Hitachi, Ibaraki, Japan) at ×3000 magnification. Starch granules were spread on double-adhesive carbon tapes fastened on an aluminum stub, and coated with a thin film of gold. The images were examined at an accelerating voltage of 3.0 kV.

2.5 X-ray diffraction analysis (X-RD)

Starch samples were moisture equilibrated in a desiccator with saturated NaCl solution for 7 d at room temperature and analyzed by a Bruker X-ray diffractometer (Bruker AXS Inc., Germany) as described by Chen, Ren, Zhang, Tong, and Rashed (2015).

The percentage relative crystallinity (RC) was calculated by using Jade 6.5 software according to the following formula.

$$RC = \frac{A_c}{A_c + A_a} \times 100\% \quad (2)$$

where A_a and A_c represent the areas in the diffractogram of amorphous and crystalline regions, respectively.

2.6 Small angle X-ray scattering (SAXS)

Starch pretreatment was performed according to Lan et al. (2016) with slight modifications. Briefly, starch was suspended in deionized water with a mass ratio of 1:3, and the slurries were shaken overnight at room temperature at 300 rpm to achieve equilibrium. Before the experiment, starch slurries were centrifuged at 8000×g for 10 min, and the precipitates were placed on the sample holder. The scattering patterns were obtained with a Xeuss 3.0 C SAXS instrument (Xenocs S.A.S, France) using a beam wavelength of λ = 1.542 nm. The sample-detector distance was 1070 mm, covering q values between 0.01 and 0.2 $Å^{-1}$, and the exposure time was 60 s.

The fractal structures of starch granules can be described by the fractal dimension D, which is calculated according to the power-law equation:

$$I(q) \sim q^{-\alpha} \quad (3)$$

where q is the scattering vector; I(q) is the scattering intensity and α is an exponent that is the slope of the linear fitting of the SAXS scattering curve in the low q range under the double logarithmic axis (Suzuki, Chiba, & Yano, 1997).

To further investigate the lamellar structure of starch granules, SAXS curves were transformed using the one-dimensional linear correlation function γ(x):

$$\gamma(x) = \frac{\int_0^\infty I(q)q^2 cos(qx)dq}{\int_0^\infty I(q)q^2 dq} \quad (4)$$

where x is the distance in real space, and the denominator is the scattering invariant (Lan et al., 2016).

2.7 Determination of amylose content

The amylose content of all starch samples was determined using the lectin concanavalin A (Con A) method provided as a commercial kit, assays K-AMYL from Megazyme (Gibson, Solah, & McCleary, 1997). In this method, the role of Con A is to precipitate amylopectin by forming a complex. After hydrolysis by a mixture of amyloglucosidase and α-amylase, the mass ratio of amylose in the total starch was obtained from the conversion to glucose quantified with the GOPOD method.

2.8 High performance anion exchange chromatography (HPAEC)

The chain length distribution of all starch samples was obtained by high-performance anion exchange chromatography with pulsed amperometric detection (HPAEC-PAD) (ICS-5000+, Thermo Fisher Scientific, USA) as described by Ji et al. (2019). Each sample (10 mg) was poured into 5 mL 50 mM sodium acetate pH 4.5 and boiled for 30 min to complete the gelatinization. The gelatinized starch was placed in an enzyme reactor to let the temperature decrease to 40℃ and isoamylase and pullulanase were added to fully debranch the samples during 12 h. The enzymes were inactivated by boiling for 10 min and followed by centrifugation (10,000×g, 10 min). The supernatant was filtered through 0.22 μm membrane filter and injected (20 μL) onto a CarboPac PA200 column at 30 °C, and elution at a flow rate of 0.4 mL/min using isocratic 150 mM NaOH and a linear gradient NaOAc (0-400 mM) as mobile phase.

2.9 Swelling power

Swelling power was determined with 10% (w/v) starch slurry according to the method of Li, He, Dhital, Zhang, and Huang (2017). The slurry was heated at 60℃ with shaking for 30 min, and centrifugated at 4000×g for10 min. The swelling power was described as follows:

$$SP = {}^{M_1}/_{M_0} \quad (5)$$

where M_1 is the weight of supernatant and M_0 the mass of the dry weight of the starch samples.

2.10 Differential scanning calorimetry (DSC)

The thermal and retrogradation property of all starch samples were measured by a DSC7000 calorimeter (HITACHI, Japan). Briefly, from 2 to 4 mg starch powder was placed in an aluminum pan, and twice the mass of deionized water was added. The sample pans were sealed tightly, and equilibrated over-night. The heating procedure is according to the description of Wang et al. (2020). An empty

aluminum pan was used as reference. After gelatinization, sample pans were placed in a plastic valve bag and stored at 4℃ for 7, 14, 21, and 28 d, and rescanned using the same heating procedure.

2.11 Rapid viscosity analysis (RVA)

Rapid visco-analyser (RVA-RECHMASTER, Newport Scientific Pty. Ltd, Sidney, Australia) was used to monitor the pasting properties of all starch samples. Briefly, starch powders were poured in an aluminum canister, mixed with deionized water up to 10% (w/w, dry basis) and stirred with a plastic paddle to avoid generation of lumps (Li, Li, & Guo, 2020). The pasting parameters of the starch slurry were determined according to the manner of Chen et al. (2015). Pasting parameters were recorded and expressed in cP units.

2.12 Statistical analysis

All data were reported as means ± standard deviation with triplicate experiments unless otherwise specified. Statistical significance was assessed with one-way analysis of variance (ANOVA) using SPSS 20.0 (SPSS Inc., Chicago, USA) for windows program. p value <0.05 was considered to be statistically significant throughout the study.

3. Results and discussion

3.1 Morphological characteristics

The morphological properties of native, control and MA treated wheat starch granules are displayed in Fig. 1. The surface of native starch granules was smooth and no obvious wrinkle or depression existed. However, the control samples exhibited a rough surface but no cracks or pits appeared. The polarized light microscope pictures (Fig. 1A-G) demonstrated that all samples retained the Maltese cross centered at the hilum illustrating the birefringence of crystalline starch indicating that the crystalline structure of the starch granules was not completely destroyed by the MA treatment. Compared with the native and control samples, the MA treatment changed the surface microstructure of the starch granules significantly, and the amount of MA added, in other words the DH considerably affects the granule morphology. Surface erosion and pits were observed in samples with MA treated as shown in Fig. 1c-g. With extended treatment, the pitting area became larger and developed into grooves and cracks on the surface. Besides, no formation of pores or channels was observed on the granule surface. These figures indicated that MA treated wheat starch granules by surface pitting, follows an “outside-in” hydrolysis pattern. This is in contrast to MA hydrolyzing corn starch granules, which yield an “inside-out” pattern by generating numerous pores and channels from the granule surface to the hilum followed by entering and acting on

the interior of the granule (Zhong et al., 2021). The difference in digestion patterns could be attribute to the different surface microstructure of these two starches. Native corn starch granules possess irregular shapes with sharp edges, a rough surface and small pores connecting internal cavity to the external surface. These pores and channels were suspected to be related to the "inside-out" hydrolysis pattern (Dhital, Shrestha, & Gidley, 2010). However, the surface of wheat starch granules were mostly smooth and micropores could only be discovered at the equatorial circular depression of the tabular granules (Zan et al., 2021). This structural feature of wheat starch might restrain the penetration of MA into the starch granules and thus influences the MA reactivity.

3.2 Crystalline structure

To further understand the impact of MA hydrolysis on crystalline and amorphous regions of starch granules, an X-ray diffractometer was used to determine the variation of crystallinity. As illustrated in Fig. 2, native wheat starch exhibited an A-type pattern with sharp diffraction peaks at 2θ around 15°, 17°, 18° and 23°, with the relative crystallinity of 25.83%. Notably, all samples displayed a weak peak at 2θ of 20°, which could be attributed to amylose-lipid complex (Zobel, 1988). The relative crystallinity of the control sample was lower than that of the native starch, indicating damage of starches at the crystalline structure level (Zhong et al., 2021). MA treatment did not alert the crystalline pattern of the starches, while the relative crystallinity increased compared to control samples. This phenomenon is caused by the hydrolytic activities in amorphous regions and therefore increased the ratio of crystalline structure (Zhao et al., 2018). It is noticed that the relative crystallinity advanced continually until the amount of MA reached 10 U/g, and decreased slightly as it was increased to 15 U/g. This result indicated that MA could as well disrupt crystalline regions in starch granules, resulting in the decline of the percentage of crystalline regions.

3.3 Lamellar structure and fractal characteristics

The lamellar structures and fractal characteristics of starches were further investigated by SAXS. As illustrated in Fig. 3A, all samples displayed an obvious scattering peak at the q value of approximately 0.06 $Å^{-1}$, indicating an average thickness of the semi-crystalline growth rings in starch granules of 9~10 nm (Kuang et al., 2017). The scattering peak intensity is determined by the amount of well-organized semi-crystalline structures and/or by the electron density differences between crystalline and amorphous lamellae in starches (Yuryev et al., 2004). MA treatment led to a reduction in peak intensity, which resulted from hydrolysis by MA destroying the granule structures and declining the difference in electron

density between the two types of lamellae. In order to make the scattering peak more distinct and further analyze the SAXS curve, we performed a Lorentz correction. The profiles are shown in Fig. 3B. The intensity of each peak displayed similar trends as in Fig. 3A. The values of scattering vector corresponding to the peak vertices (q_1) and the values of D_{Bragg} calculated from q_1 by Bragg's law ($D_{Bragg}=2\pi/q_1$) are shown in Table 1. Native wheat starch granules displayed the biggest D_{Bragg} of 9.98 nm, and MA treatment bring about a decrease in D_{Bragg} as shown in Table 1.

To further investigate the lamellar structure of starch granules, the one-dimensional linear correlation functions were measured. As shown in Fig. 3C inset, based on the function curve, the x value corresponding to the first maximum of the γ(x) represents the long period (d_p), the solution of linear regression in the auto correlation triangle (LRAT) at *y* equals the value of the minimum of γ(x) representing the thickness of amorphous lamellae (d_a). Therefore, the average thickness of the crystalline lamellae (d_c) equals d_p-d_a (Goderis, Reynaers, Koch, & Mathot, 1999). The lamellar structure parameters of starches calculated according to the normalized one-dimensional function in Fig. 3C are displayed in Table 1. The native wheat starch granules contain the highest d_p value of 9.10 nm. The lowest d_p belongs to 15 U/g MA treated starch granules, illustrating that the long period is shortened by MA hydrolysis. However, with the further degradation of starch granules, no uniform trend appeared in the change of d_p values. The same phenomenon was also reported by Lan et al. (2016). Moreover, MA treatment led to a decrease in d_c, indicating that the thickness of the crystal lamellae became thinner. This might be caused by MA hydrolysis of the granule crystalline region, which shortened the length of branch chains in amylopectin, and thus, shortened the length of double helices, resulting in thinning of the crystalline lamellae. However, the thickness of amorphous lamellae became thicker after MA treatment as shown in Table 1. This could be attributed to MA treatment loosening the double helices generating the increase in spacing (Lan et al., 2016). Therefore, MA could act on both crystalline and amorphous regions to digest starch granules. Furthermore, it is noticeable that the D_{Bragg} is higher than d_p in native and modified starch granules, which has been reported previously (Lan, Zhang, Wu, Xie, & Wang, 2016). Under ideal circumstances, there is a regular alternating structure between crystalline lamellae and amorphous lamellae. Only under this condition do D_{Bragg} and d_p have the same value. But actually, irregular alternating disordered structure exists in starch granules, thus D_{Bragg} is higher than d_p (Crist, 2007).

To investigate the surface smoothness and mass compactness information of starch samples, the fractal dimension was determined (Table 1). The fractal dimension of starch granules belongs to the

surface fractal structure or mass fractal structure and is determined by the value of the exponent α in Eq. (3). The inset in Fig. 3A shows the calculation of α. Depending on the fractal characteristics of the scattering object, the exponent α can take a value in the range of 1 to 4. When fractal information was obtained from scattering experiments, in other words, the linear relationship between log I(q) and log q following Eq. (3), the character of the scattering sources could be determined on the basis of α (Martin & Hurd, 1987). In the case of $3<\alpha<4$, the scattering is suggested to generate from surface roughness and is distinguished by surface fractal. The surface fractal dimension $D_s=6-\alpha$. In the case of $1<\alpha<3$, the scattering in identified due to the interior structure of objects, in which the mass fractal dimension $D_m=\alpha$ (Suzuki et al., 1997). As shown in Table 1, all samples contain an α value within 1 to 3, indicating a mass fractal dimension.

3.4 Amylose content

The amylose content of all starch samples is shown in Table 2. The native wheat starch contains 24.9% amylose. It is interesting to notice that no significant difference was observed in amylose content between native, control and MA treated wheat starch samples. Meanwhile, the DH value in Table 2 demonstrated that starch granules were degraded continuously with increasing MA dosage. Therefore, it may be that MA can degrade both amylose and amylopectin simultaneously. The same result was also reported when porcine pancreas α-amylase hydrolyzed corn starch granules (Zhang, Ao, & Hamaker, 2006). Generally, in raw starch granules, a large portion of the amylose is located in the amorphous layers of the growth rings, and amylopectin is the main component of the crystalline regions (Vamadevan & Bertoft, 2015). Previous literature suggested that compared to crystalline regions, amorphous regions of starch granules were more susceptible to attack by enzymes (Zavareze & Dias, 2011). But the data presented in the present study suggest that MA could simultaneously hydrolyze amylose and amylopectin in amorphous and crystalline regions of starch granules, which is consistent with the result in Section 3.3.

3.5 Chain structure

To further investigate the fine structure of wheat starch granules after MA hydrolysis, all starch samples after debranching for 12 h were analyzed using HPAEC. The chain length distribution could be identified into 4 groups based on the degree of polymerization (DP): fa chains (DP 6-12), fb_1 chains (DP 13-24), fb_2 chains (DP 25-36) and fb_3 chains (DP ≥ 37) (Hanashiro, Abe, & Hizukuri, 1996). As demonstrated (Table 2, Fig. 4A) the proportion of fb_1 chains was highest in the native wheat starch accounting for 47.02%. MA treatment induced a distinct increase in the percentage of very short chains

(DP≤6) accompanied by a decrease in the percentage of fa and fb chains, especially the fb_1 chains. More exactly, incubation with MA increased the proportion of DP＜9 chains from 5.43% of the control to 12.92% of the sample treated by 15 U/g MA, and the proportion of chains of DP＞9 decreased to different extent. This phenomenon could be explained by the *exo*-action of MA hydrolyzing mainly long chains, generating short chains (Grewal et al., 2015).

3.6 Gelatinization and retrogradation characteristics

The gelatinization and retrogradation parameters as deduced by DSC of native, control and MA treated wheat starches are summarized in Table 3. The gelatinization temperature of native wheat starches ranges from 58.18℃ to 68.74℃ and the gelatinization enthalpy (ΔH_g) is 7.57 J/g. The control samples exhibited higher gelatinization temperatures (T_o, T_p, T_c), especially T_o, which lowered the temperature range (T_c-T_o). This could be attributed to that incubation in excess water at 55℃ led to rearranging of part of the double helix, which reduced the ratio of crystalline defects and generated more homogenous crystallites (Jayakody & Hoover, 2008). The ΔH_g of the control is significantly lower than that of native starch, demonstrating the effect of annealing lowered the amount of molecular order by the rearrangements of the double helix (Tester & Debon, 2000), which is consistent with the X-RD result. MA treatment resulted in a slight decline of gelatinization temperatures and significantly reduced the ΔH_g, indicating that hydrolysis by MA shortened the length of the starch chains and hence shortened the length of the double helix (Guo, Tao, Cui, & Janaswamy, 2019). This is in line with the chain length distribution result.

As illustrated in Table 3, the retrogradation enthalpy (ΔH_r) of native and control samples increased from 2.63 J/g to 4.09 J/g and 3.19 J/g to 4.53 J/g, respectively, during storage from 7 to 28 d, indicating that recrystallization occurred. MA treatment significantly inhibited the retrogradation of wheat starch. The ΔH_r decreased to 0.12 J/g after storage for 28 d at 4℃ for starch treated with 15 U/g MA. This might be due to the shortened amylose chains and outer chains of amylopectin that restrained generation of double helices. The extent of starch retrogradation has a positive correlation with the proportion of amylopectin chains with DP 14-24, but a negative correlation with amylopectin chains of DP 6-9 (Grewal et al., 2015). Besides, DP 10 is the minimum chain length required to form stable double helices (Gidley & Bulpin, 1989). Furthermore, short amylopectin chains of DP 5-10 are unable to participate in formation of a stable double helix structure. Therefore these branch chains have a negative effect on the formation of ordered crystalline structures (Zhang et al., 2006). Generally, starches with short branch chains have

difficulty in retrograding during storage. The results of the chain length distribution analysis (Section 3.5) supported the inhibition of starch retrogradation as MA treatment led to an increase in the percentage of chains with DP≤9 accompanied by a decrease of long chains.

3.7 Pasting properties

The pasting curves of all starch samples are demonstrated in Fig. 5, and the corresponding parameters in Table 4. MA treatment affected the pasting behaviors of wheat starch effectively and the influence was highly dependent on the MA addition. Obviously, incubation with MA significantly reduced starch pasting parameters except for breakdown viscosity, while the control sample only showed a slight change compared to native starch. The peak viscosity is closely related to the swelling and integrity of swollen starch granules (Crosbie, 1991). This effect may arise as MA treatment damaged the structural integrity of starch granules and reduced the swelling ability (Table 2) resulting in starch granules less prone to entanglement. The peak viscosity decreased with increasing MA dosage from 2789.67 cP (NWS) to 498.81 cP (15 U/g), which is consistent with the results of the DH. Finally, viscosity increases during cooling because of the aggregation of the amylose molecules (Miles, Morris, Orford, & Ring, 1985). The decrease in final viscosity could be attributed to that MA treatment, due to shortened lengths of amylose and amylopectin branch chains reducing the entanglement between starch chains. It is worth noting that MA modification led to distinct decline in setback value, which decreased by 40 % after incubation with 2.5 U/g MA for 1 h compared to the control. This decline was pronounced with increasing DH, showing an 89% decrease by treatment with 15 U/g MA, and suggesting that the short-term retrogradation of starch was inhibited.

3.8 The relationship between degree of hydrolysis and starch retrogradation parameters

The above results illustrate that the retrogradation of wheat starch is suspended through the MA treatment. Additionally, the retrogradation extent decreased with the increase of DH. Therefore, the relationship between DH and starch retrogradation was investigated further. The setback value of MA treated wheat starch demonstrated a negative correlation with DH (R^2=0.9649) (Fig. 6A). In RVA curves, the setback value is thought to be a reflection of short-term retrogradation caused by amylose aggregation (Chen et al., 2015). The result in Fig. 6A, obtained from linear regression analysis, suggested that there is a linear relationship between DH and setback value, indicating that the short-term retrogradation of MA treated wheat starch could be predicted by monitoring the value of DH. Long amylose chains contain more binding points, prone to reassociate with each other through hydrogen bonds to generate more

stable double helices (Tao, Li, Yu, Gilbert, & Li, 2019). Shortening the length of amylose chains could reduce their tendency to entangle with each other. Hence, the decrease in setback value resulted from the degradation of amylose at molecular level by MA hydrolysis. Furthermore, it demonstrated that MA can simultaneously hydrolyze amylose and amylopectin (Section 3.4), therefore DH could represent the extent of amylose chain length shortening. In other words, the higher the DH, the less easy for amylose to entangle and rearrange due to shortening. Consequently, the setback value was decreased.

The relationship between DH and ΔH_r is demonstrated in Fig. 6B. It was observed that the ΔH_r of MA treated wheat starch after aging for 7, 14, 21, and 28 d at 4℃ also showed negative correlation with DH, R^2 equals 0.9385, 0.9797, 0.9871, and 0.9693, respectively. Gelatinized starches begin to reassemble and rearrange into microcrystalline forms through formation of hydrogen bonds contributing to a more ordered or crystalline structure during storage (Wang et al., 2021). The ΔH_r obtained by DSC is a measure of the extent of starch retrogradation, especially amylopectin retrogradation. The result in Fig. 6B, obtained from linear regression analysis, suggests that long-term retrogradation of MA modified wheat starch could be predicted by monitoring the DH. Previous reports suggested that β-limit dextrin showed no endothermic peaks in DSC tests after storage at 4℃ for 7 d (Klucinec & Thompson, 2002), and starch with higher proportion of long B chains is more liable to occur in intermolecular reassociations (Klucinec & Thompson, 1999). Moreover, it has been proven that there is a linear correlation between long-term retrogradation and average chain length of amylopectin (Li et al., 2016). Data in Section 3.6 exhibited that with the increase of DH, the proportion of short chain in amylopectin increased and the proportion of long chain decreased. Therefore, it makes sense to yield a linear correlation between long retrogradation enthalpy and DH.

4. Conclusions

MA was used to modify granular wheat starch at sub-gelatinization temperature to investigate the relationship between DH and retrogradation. SEM photos revealed the “surface erosion” pattern on wheat starch granules by MA. MA was able to act on both amorphous and crystalline regions. The amylose content of all samples displayed no significant difference, demonstrating that MA can simultaneously digest amylose and amylopectin in raw wheat starch. MA treatment resulted in generation of a large proportion of short chains (DP≤9) accompanied by decrease in long chains in amylopectin. As a consequence, pasting viscosity and gelatinization enthalpy both decreased. The short- and long-term retrogradation of MA treated wheat starch was inhibited as illustrated by the setback value in RVA curves

and DSC measurement. Moreover, the retrogradation property (setback value and retrogradation enthalpy) of starch and DH exhibited a linear relationship, indicating that retrogradation of MA modified starch can be predicted by monitoring the extent of hydrolysis. This correlation could be used to guide the utilization of MA in starch customization and improvement of anti-staling ability of starchy foods.

CRediT authorship contribution statement

Yitan Zhai: Investigation, Writing, Validation, Conceptualization. **Xiaoxiao Li:** Review & editing. **Yuxiang Bai:** Review & editing, Project administration, Funding acquisition, Supervision. **Zhengyu Jin:** Funding acquisition. **Brite Svensson:** Review & editing.

Declarations of competing interest

No conflicts of interest are declared for any of the authors.

Acknowledgements

This work was supported by National Natural Science Foundation of China (grant number 32072268), Agricultural Science and Technology Independent Innovation Fund of Jiangsu Province (grant number CX(17)2022) and National First-Class Discipline Program of Food Science and Technology (JUFSTR20180203).

References

Adebowale, K. O., & Lawal, O. S. (2003). Microstructure, physicochemical properties and retrogradation behaviour of Mucuna bean (Mucuna pruriens) starch on heat moisture treatments. *Food Hydrocolloids, 17*(3), 265-272.

Chen, L., Ren, F., Zhang, Z., Tong, Q., & Rashed, M. M. A. (2015). Effect of pullulan on the short-term and long-term retrogradation of rice starch. *Carbohydrate Polymers, 115*, 415-421.

Chen, X., Zhang, L., Li, X., Qiao, Y., Zhang, Y., Zhao, Y., Chen, J., Xianfeng, Y., Huang, Y., Li, Z., & Cui, Z. (2020). Impact of maltogenic alpha-amylase on the structure of potato starch and its retrogradation properties. *International Journal of Biological Macromolecules, 145*, 325-331.

Crist, B. (2007). Analysis of Small-Angle X-Ray Scattering Patterns. *Journal of Macromolecular Science, Part B, 39*(4), 493-518.

Crosbie, G. B. (1991). The relationship between starch swelling properties, paste viscosity and boiled noodle quality in wheat flours. *Journal of Cereal Science, 13*(2), 145-150.

Dauter, Z., Dauter, M., Brzozowski, A. M., Christensen, S., Borchert, T. V., Beier, L., Wilson, K. S., & Davies, G. J. (1999). X-ray structure of Novamyl, the five-domain "maltogenic" alpha-amylase from Bacillus stearothermophilus: Maltose and acarbose complexes at 1.7 angstrom resolution. *Biochemistry, 38*(26), 8385-8392.

Dhital, S., Shrestha, A. K., & Gidley, M. J. (2010). Relationship between granule size and in vitro digestibility of maize and potato starches. *Carbohydrate Polymers, 82*(2), 480-488.

Fu, Z., Chen, J., Luo, S.-J., Liu, C.-M., & Liu, W. (2015). Effect of food additives on starch retrogradation: a review. *Starch/Staerke, 67*(1-2), 69-78.

Gibson, T. S., Solah, V. A., & McCleary, B. V. (1997). A procedure to measure amylose in cereal starches and flours with concanavalin A. *Journal of Cereal Science, 25*(2), 111-119.

Gidley, M. J., & Bulpin, P. V. (1989). Aggregation of amylose in aqueous systems: the effect of chain length on phase behavior and aggregation kinetics. *Macromolecules, 22*(1), 341-346.

Goderis, B., Reynaers, H., Koch, M. H. J., & Mathot, V. B. F. (1999). Use of SAXS and linear correlation functions for the determination of the crystallinity and morphology of semi-crystalline polymers. Application to linear polyethylene. *Journal of Polymer Science Part B-Polymer Physics, 37*(14), 1715-1738.

Grewal, N., Faubion, J., Feng, G., Kaufman, R. C., Wilson, J. D., & Shi, Y. C. (2015). Structure of Waxy

411 Maize Starch Hydrolyzed by Maltogenic alpha-Amylase in Relation to Its Retrogradation. *Journal of*
412 *Agricultural and Food Chemistry, 63*(16), 4196-4201.
413 Gui, Y., Zou, F., Li, J., Zhu, Y., Guo, L., & Cui, B. (2021). The structural and functional properties of
414 corn starch treated with endogenous malt amylases. *Food Hydrocolloids, 117*, 106722-106722.
415 Guo, L., Tao, H., Cui, B., & Janaswamy, S. (2019). The effects of sequential enzyme modifications on
416 structural and physicochemical properties of sweet potato starch granules. *Food Chemistry, 277*, 504-
417 514.
418 Hanashiro, I., Abe, J., & Hizukuri, S. (1996). A periodic distribution of the chain length of amylopectin
419 as revealed by high-performance anion-exchange chromatography. *Carbohydrate research, 283*, 151-
420 159.
421 Jayakody, L., & Hoover, R. (2008). Effect of annealing on the molecular structure and physicochemical
422 properties of starches from different botanical origins – A review. *Carbohydrate Polymers, 74*(3), 691-
423 703.
424 Ji, H., Bai, Y., Li, X., Wang, J., Xu, X., & Jin, Z. (2019). Preparation of malto-oligosaccharides with
425 specific degree of polymerization by a novel cyclodextrinase from Palaeococcus pacificus. *Carbohydrate*
426 *Polymers, 210*, 64-72.
427 Klucinec, J. D., & Thompson, D. B. (1999). Amylose and amylopectin interact in retrogradation of
428 dispersed high-amylose starches. *Cereal Chemistry, 76*(2), 282-291.
429 Klucinec, J. D., & Thompson, D. B. (2002). Amylopectin nature and amylose-to-amylopectin ratio as
430 influences on the behavior of gels of dispersed starch. *Cereal Chemistry, 79*(1), 24-35.
431 Kuang, Q., Xu, J., Liang, Y., Xie, F., Tian, F., Zhou, S., & Liu, X. (2017). Lamellar structure change of
432 waxy corn starch during gelatinization by time-resolved synchrotron SAXS. *Food Hydrocolloids, 62*, 43-
433 48.
434 Lan, X., Xie, S., Wu, J., Xie, F., Liu, X., & Wang, Z. (2016). Thermal and enzymatic degradation induced
435 ultrastructure changes in canna starch: Further insights into short-range and long-range structural orders.
436 *Food Hydrocolloids, 58*, 335-342.
437 Lan, X., Zhang, J., Wu, J., Xie, F., & Wang, Z. (2016). Application of two-phase lamellar model to study
438 the ultrastructure of annealed canna starch: A comparison with linear correlation function. *International*
439 *Journal of Biological Macromolecules, 93*, 1210-1216.
440 Li, H., Li, J., & Guo, L. (2020). Rheological and pasting characteristics of wheat starch modified with

sequential triple enzymes. *Carbohydrate Polymers, 230*.

Li, P., He, X., Dhital, S., Zhang, B., & Huang, Q. (2017). Structural and physicochemical properties of granular starches after treatment with debranching enzyme. *Carbohydrate Polymers, 169*, 351-356.

Li, W., Li, C., Gu, Z., Qiu, Y., Cheng, L., Hong, Y., & Li, Z. (2016). Relationship between structure and retrogradation properties of corn starch treated with 1,4-α-glucan branching enzyme. *Food Hydrocolloids, 52*, 868-875.

Lombard, V., Golaconda Ramulu, H., Drula, E., Coutinho, P. M., & Henrissat, B. (2014). The carbohydrate-active enzymes database (CAZy) in 2013. *Nucleic Acids Research, 42*(D1), D490-D495.

M. DuBois, K. A. Gilles, J. K. Hamilton, P. A. Rebers, & F. Smith. (1956). Colorimetric Method for Determination of Sugars and Related Substances. *Analytical Chemistry, 28*(3), 350-356.

Martin, J. E., & Hurd, A. J. (1987). Scattering from fractals. *Journal of Applied Crystallography, 20*(2), 61-78.

Miles, M. J., Morris, V. J., Orford, P. D., & Ring, S. G. (1985). The roles of amylose and amylopectin in the gelation and retrogradation of starch. *Carbohydrate research, 135*(2), 271-281.

Park, S., & Kim, Y.-R. (2021). Clean label starch: production, physicochemical characteristics, and industrial applications. *Food Science and Biotechnology, 30*(1), 1-17.

Suzuki, T., Chiba, A., & Yano, T. (1997). Interpretation of small angle X-ray scattering from starch on the basis of fractals. *Carbohydrate Polymers, 34*(4), 357-363.

Tao, K., Li, C., Yu, W., Gilbert, R. G., & Li, E. (2019). How amylose molecular fine structure of rice starch affects functional properties. *Carbohydrate Polymers, 204*, 24-31.

Tester, R. F., & Debon, S. J. J. (2000). Annealing of starch - a review. *International Journal of Biological Macromolecules, 27*(1), 1-12.

Vamadevan, V., & Bertoft, E. (2015). Structure-function relationships of starch components. *Starch-Starke, 67*(1-2), 55-68.

Wang, Y., Chen, L., Yang, T., Ma, Y., McClements, D. J., Ren, F., Tian, Y., & Jin, Z. (2021). A review of structural transformations and properties changes in starch during thermal processing of foods. *Food Hydrocolloids, 113*.

Wang, Y., Li, X., Ji, H., Zheng, D., Jin, Z., Bai, Y., & Svensson, B. (2020). Thermophilic 4-alpha-Glucanotransferase from Thermoproteus Uzoniensis Retards the Long-Term Retrogradation but Maintains the Short-Term Gelation Strength of Tapioca Starch. *Journal of Agricultural and Food*

Chemistry, 68(20), 5658-5667.

Yang, H., Tang, M., Wu, W., Ding, W., Ding, B., & Wang, X. (2021). Study on inhibition effects and mechanism of wheat starch retrogradation by polyols. *Food Hydrocolloids, 121*, 106996.

Yuryev, V. P., Krivandin, A. V., Kiseleva, V. I., Wasserman, L. A., Genkina, N. K., Fornal, J., Blaszczak, W., & Schiraldi, A. (2004). Structural parameters of amylopectin clusters and semi-crystalline growth rings in wheat starches with different amylose content. *Carbohydrate research, 339*(16), 2683-2691.

Zan, K., Wang, J., Ren, F., Yu, J., Wang, S., Xie, F., & Wang, S. (2021). Structural disorganization of cereal, tuber and bean starches in aqueous ionic liquid at room temperature: Role of starch granule surface structure. *Carbohydrate Polymers, 258*.

Zavareze, E. d. R., & Dias, A. R. G. (2011). Impact of heat-moisture treatment and annealing in starches: A review. *Carbohydrate Polymers, 83*(2), 317-328.

Zhang, G., Ao, Z., & Hamaker, B. R. (2006). Slow digestion property of native cereal starches. *Biomacromolecules, 7*(11), 3252-3258.

Zhao, A.-Q., Yu, L., Yang, M., Wang, C.-J., Wang, M.-M., & Bai, X. (2018). Effects of the combination of freeze-thawing and enzymatic hydrolysis on the microstructure and physicochemical properties of porous corn starch. *Food Hydrocolloids, 83*, 465-472.

Zhong, Y., Keeratiburana, T., Kain Kirkensgaard, J. J., Khakimov, B., Blennow, A., & Hansen, A. R. (2021). Generation of short-chained granular corn starch by maltogenic α-amylase and transglucosidase treatment. *Carbohydrate Polymers, 251*.

Zobel, H. F. (1988). Starch crystal transformations and their industrial importance. *Starch/Staerke, 40*(1), 1-7.

493 ■ **Tables**

494 ■ **Table 1.** The lamellar parameters and fractal features of native, control and MA treated wheat starch granules

Sample	q_1 ($Å^{-1}$)	D_{Bragg} (nm)	Lamellar parameter			Fractal features		
			d_p (nm)	d_c (nm)	d_a (nm)	α	D_m	R^2
NWS	0.062969	9.98	9.10	5.52	3.58	1.99	1.80	0.995
Control	0.063553	9.88	9.04	5.35	3.69	2.24	2.23	0.999
2.5 U/g	0.064124	9.80	9.01	5.04	3.97	2.31	2.31	0.999
5 U/g	0.064124	9.80	9.03	5.09	3.94	2.30	2.27	0.999
7.5 U/g	0.063553	9.89	9.01	5.05	3.96	2.28	2.31	0.999
10 U/g	0.063267	9.93	9.02	5.09	3.93	2.25	2.27	0.999
15 U/g	0.063553	9.89	8.98	5.04	3.94	2.27	2.31	0.999

495

496

497 ■ **Table 2.** Degree of hydrolysis, amylose content, swelling power and chain length distribution of native, control and MA treated starches

Sample	DH (%)	Amylose content (%)	Swelling power (g/g)	Chain length distribution (%)				
				DP＜6	DP 7-12	DP 13-24	DP 25-36	DP＞37
NWS	- -	24.9±1.5^{a}	4.58±0.21^{a}	6.82	27.87	45.49	14.77	5.05
Control	- -	23.4±1.3^{a}	4.17±0.31^{ab}	5.43	28.28	46.98	14.85	4.46
2.5 U/g	10.11±0.43^{e}	24.5±1.1^{a}	3.91±0.31^{b}	9.16	27.25	44.62	14.26	4.71
5 U/g	12.66±0.31^{d}	23.8±1.8^{a}	3.92±0.34^{b}	9.51	27.19	44.53	14.13	4.64
7.5 U/g	14.63±0.54^{c}	23.3±0.2^{a}	3.88±0.36^{b}	10.45	27.17	43.75	14.07	4.56
10 U/g	17.31±0.83^{b}	22.9±1.8^{a}	3.67±0.34^{b}	11.51	26.87	43.38	13.83	4.41
15 U/g	21.13±0.69^{a}	24.2±1.7^{a}	3.70±0.39^{b}	12.92	26.68	42.22	13.79	4.39

498 Values followed by different letters within a column are significantly different ($p < 0.05$).

499

500 ■ **Table 3.** Gelatinization properties and retrogradation enthalpy of native, control and MA treated wheat starches

Sample	Gelatinization of starch					Retrogradation enthalpy ΔH_r (J/g)			
	T_o (℃)	T_p (℃)	T_c (℃)	T_c-T_o (℃)	ΔH_g (J/g)	7d	14d	21d	28d
NWS	58.18±0.22^{c}	63.80±0.40^{c}	68.74±0.30^{d}	10.56±0.37^{a}	7.57±0.27^{a}	2.63±0.30^{b}	3.21±0.15^{b}	3.68±0.27^{b}	4.09±0.42^{b}
Control	65.53±0.21^{a}	67.58±0.13^{a}	70.84±0.11^{a}	5.31±0.29^{b}	6.58±0.29^{b}	3.19±0.013^{a}	3.71±0.31^{a}	4.33±0.06^{a}	4.53±0.30^{a}
2.5 U/g	65.35±0.17^{ab}	67.48±0.14^{ab}	70.53±0.20^{ab}	5.18±0.11^{b}	5.87±0.12^{c}	0.46±0.04^{c}	0.54±0.02^{c}	0.59±0.04^{c}	0.69±0.16^{c}
5 U/g	65.34±0.22^{ab}	67.22±0.19^{ab}	70.42±0.18^{bc}	5.08±0.12^{b}	5.74±0.06^{cd}	0.27±0.07^{cd}	0.41±0.09^{cd}	0.45±0.09^{cd}	0.49±0.06^{cd}
7.5 U/g	65.21±0.11^{b}	67.17±0.15^{b}	70.28±0.05^{bc}	5.07±0.14^{b}	5.69±0.13^{cd}	0.24±0.04^{de}	0.28±0.06^{de}	0.33±0.01^{de}	0.37±0.03^{cd}
10 U/g	65.16±0.10^{b}	67.16±0.14^{b}	70.18±0.10^{b}	5.02±0.18^{b}	5.54±0.10^{de}	0.12±0.02^{de}	0.19±0.06^{de}	0.24±0.03^{ef}	0.28±0.04^{d}
15 U/g	65.26±0.07^{ab}	67.52±0.14^{ab}	70.58±0.18^{ab}	5.31±0.11^{b}	5.36±0.04^{e}	0.04±0.01^{e}	0.07±0.03^{e}	0.09±0.01^{f}	0.12±0.03^{d}

501 Values followed by different letters within a column are significantly different ($p < 0.05$).

502

503 ■ **Table 4.** Pasting properties of native, control and MA treated starches

Sample	Peak viscosity (cP)	Trough viscosity (cP)	Final viscosity (cP)	Breakdown viscosity (cP)	Setback viscosity (cP)
NWS	2789.67±23.45^{a}	1891.79±13.68^{a}	3927.46±31.70^{a}	897.89±9.79^{a}	2035.68±18.02^{a}
Control	2443.04±19.22^{b}	1830.40±33.10^{b}	3924.98±10.96^{a}	612.64±13.88^{b}	2094.58±22.14^{b}
2.5 U/g	1165.52±15.29^{c}	593.80±6.88^{c}	1879.34±30.03^{b}	571.72±8.81^{c}	1285.54±23.31^{c}
5 U/g	1148.46±8.20^{c}	529.79±20.69^{d}	1703.70±45.06^{c}	618.67±12.50^{b}	1173.91±24.38^{d}
7.5 U/g	897.46±18.69^{d}	400.98±31.97^{e}	1200.59±5.91^{d}	496.48±13.29^{d}	799.61±26.09^{e}
10 U/g	853.34±22.55^{e}	361.34±3.53^{f}	1052.22±8.67^{e}	491.99±19.07^{d}	690.88±5.16^{f}
15 U/g	498.81±9.84^{f}	168.76±3.64^{g}	401.07±4.49^{f}	330.05±6.33^{e}	232.32±1.37^{g}

504 Values followed by different letters within a column are significantly different ($p < 0.05$).

505

506 ■ **Figure Captions**

507 ■ **Fig. 1.** Morphological characteristic of (A, a) native wheat starch, (B, b) control, (C, c) – (G, g)
508 starches treated with MA at a dosage of 2.5, 5, 7.5,10, and 15 U/g, respectively.

509 ■ **Fig. 2.** X-ray diffraction patterns of (a) native wheat starch, (b) control, (c) – (g) starches treated
510 with MA at a dosage of 2.5, 5, 7.5,10, and 15 U/g, respectively.

511 ■ **Fig. 3.** Small angle X-ray scattering patterns. (A) Double-logarithmic SAXS patterns. Inset shows
512 how α was calculated, (B) Lorentz corrected SAXS patterns, (C) One-dimensional linear
513 correlation functions. Inset shows how the lamellar structure parameters were calculated.

514 ■ **Fig. 4.** Chain length distribution analysis. (A) Chain length distribution profile of native wheat
515 starch. (B)–(F) Chain length distribution profiles (bar graph) and difference plots (line graph)
516 relative to the control of starches treated with MA at a dosage of 2.5, 5, 7.5,10, and 15 U/g,
517 respectively.

518 ■ **Fig. 5.** RVA curves of the native and MA modified starch dispersions.

519 ■ **Fig. 6.** Relationship between degree of hydrolysis and retrogradation of wheat starch treated with
520 MA. (A) Relationship between DH and setback values, (B) relationship between DH and ΔH_r.

521

522 ■ **Fig. 1**

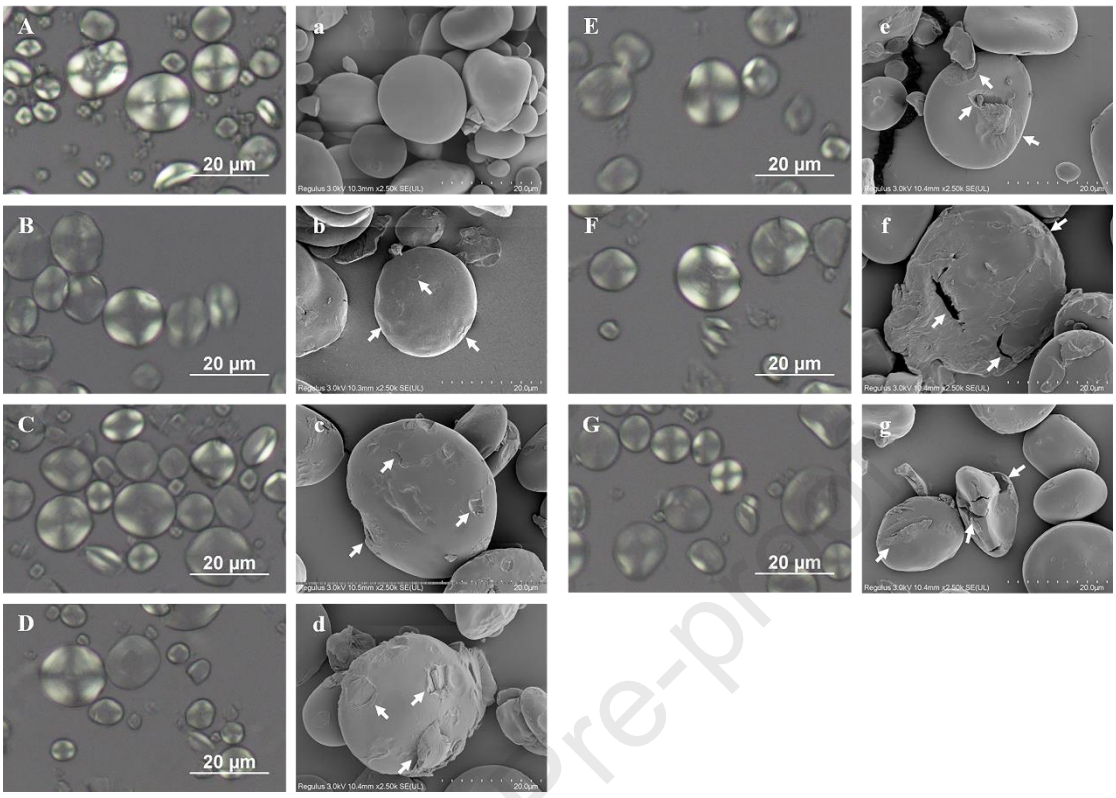

523

524

525 ■ **Fig. 2**

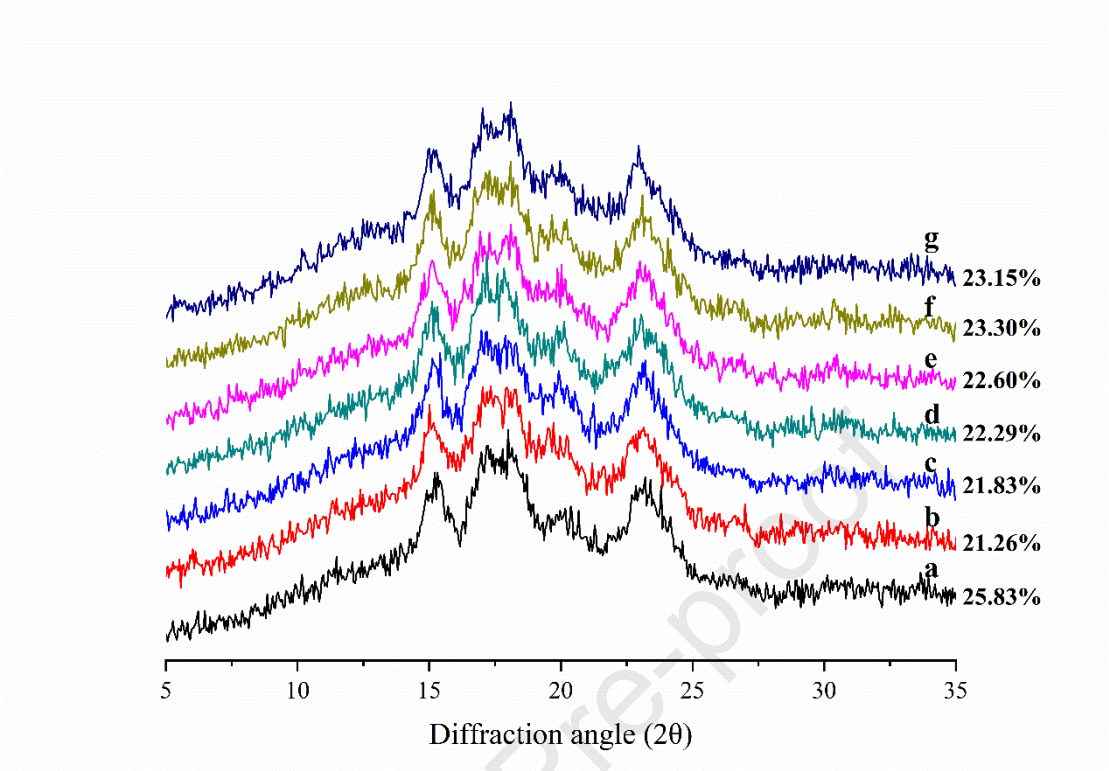

526

527

528 ■ **Fig. 3**

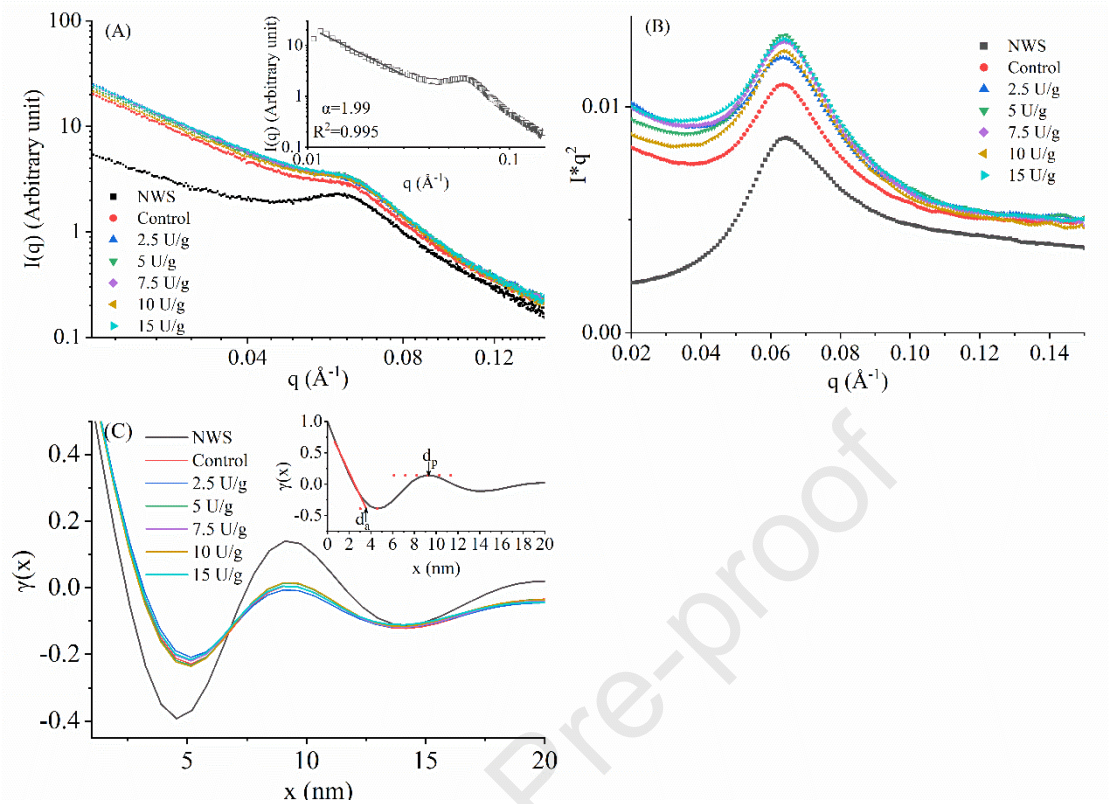

529

530

531 ■ **Fig. 4**

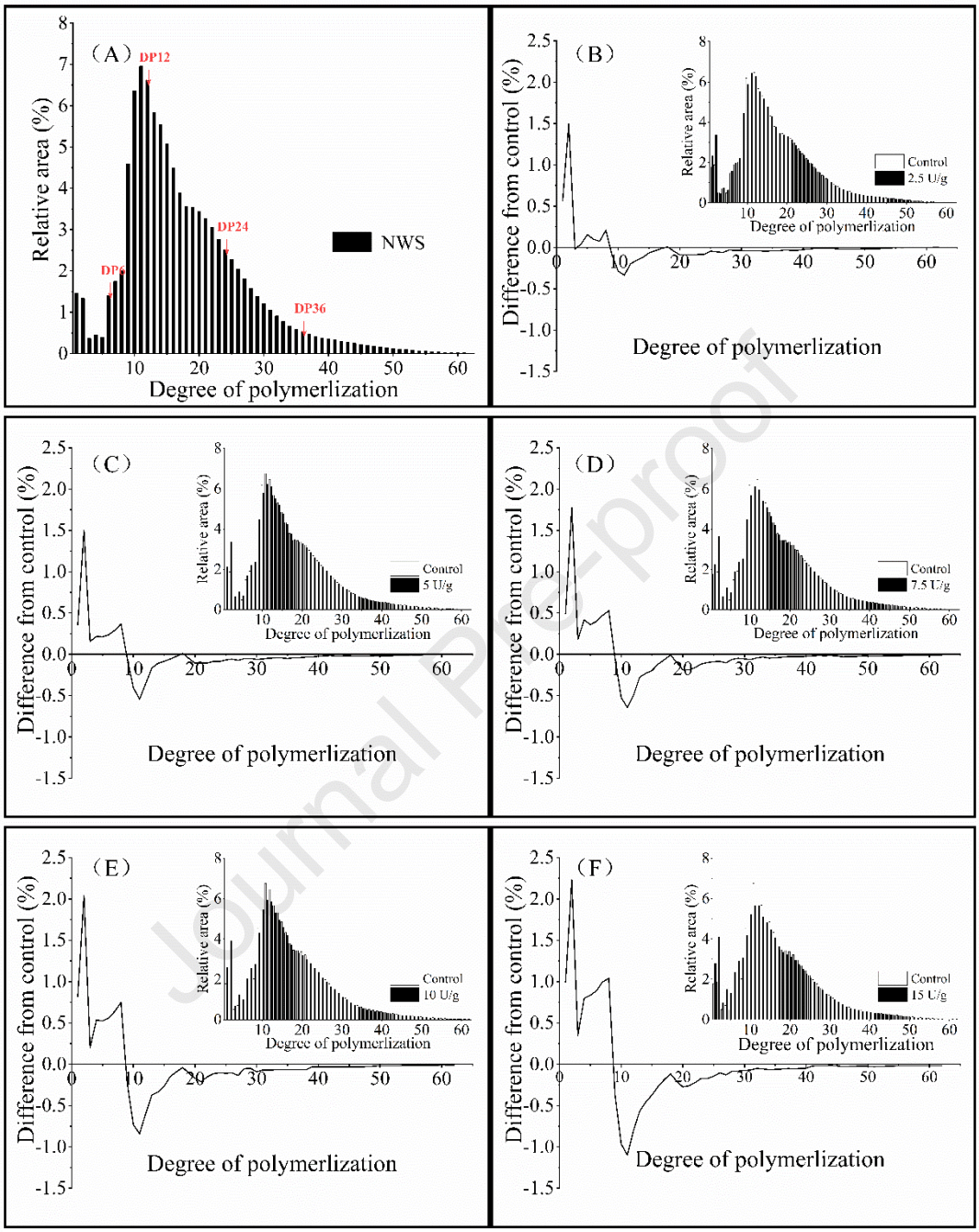

532

533

534 ■ **Fig. 5**

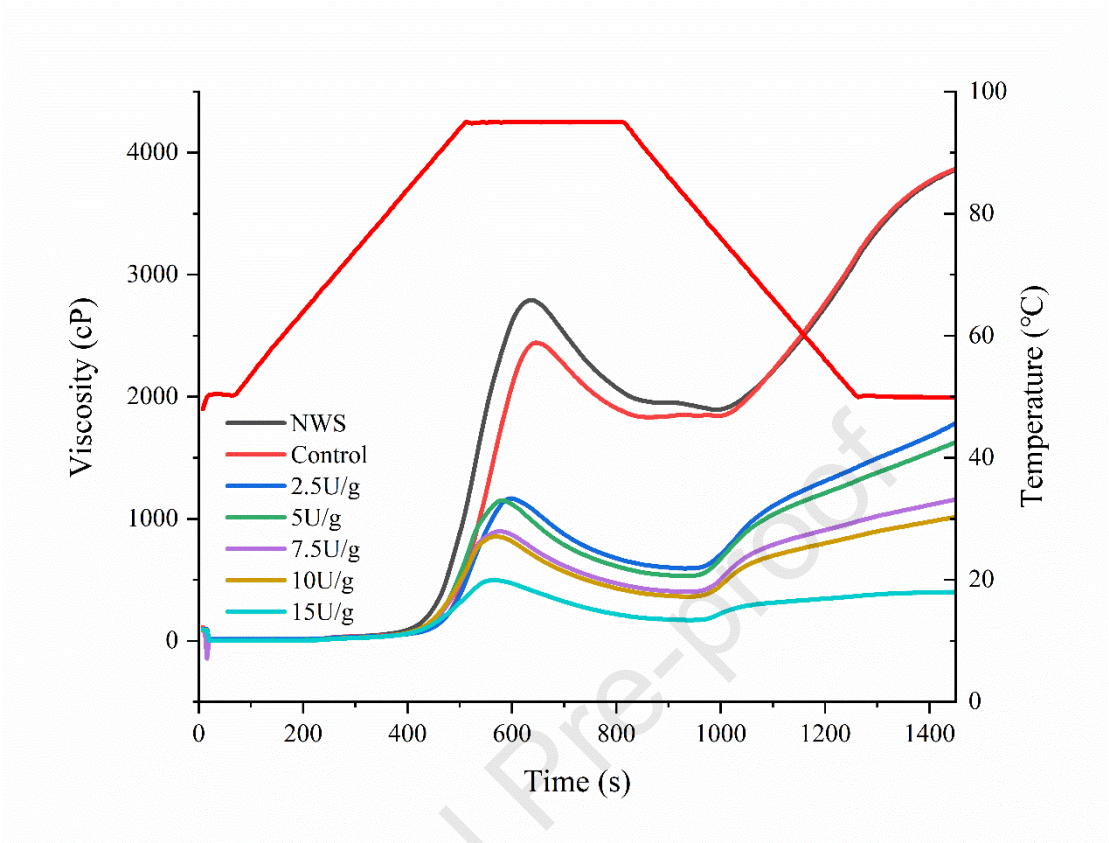

535

536

537 ■ **Fig. 6**

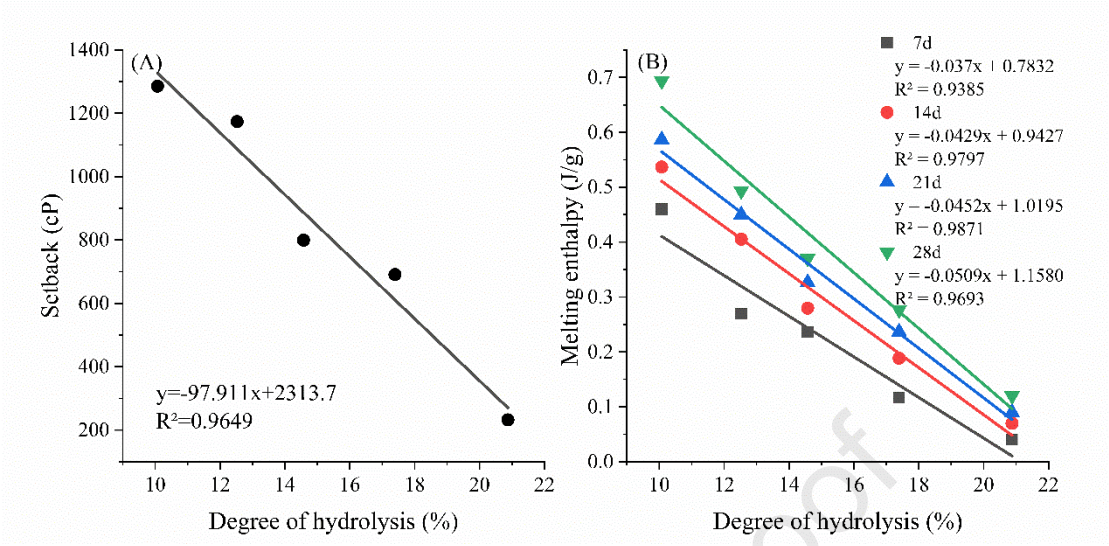

538

- Maltogenic α-amylase (MA) effectively modified wheat starch granules.
- MA could act on both amorphous and crystalline regions in wheat starch granules.
- MA treatment inhibited the short- and long-term retrogradation of wheat starch.
- The setback value and retrogradation enthalpy of MA treated wheat starch showed linear correlation with the degree of hydrolysis.

Declaration of interests

☒ The authors declare that they have no known competing financial interests or personal relationships that could have appeared to influence the work reported in this paper.

☐The authors declare the following financial interests/personal relationships which may be considered as potential competing interests: